JPn Neuroscience

The Journal of Physiology

J Physiol 594.1 (2016) pp 207–221

Ageing-related changes in GABAergic inhibition in mouse auditory cortex, measured using *in vitro* flavoprotein autofluorescence imaging

K. A. Stebbings[1], H. W. Choi[2], A. Ravindra[2], D. M. Caspary[3], J. G. Turner[3,4] and D. A. Llano[1,2]

[1] *Neuroscience Program, University of Illinois at Urbana-Champaign, IL, USA*
[2] *Department of Molecular and Integrative Physiology, University of Illinois at Urbana-Champaign, IL, USA*
[3] *Department of Pharmacology, Southern Illinois University College of Medicine, IL, USA*
[4] *Department of Psychology, Illinois College, IL, USA*

Key points

- Ageing is associated with hearing loss and changes in GABAergic signalling in the auditory system.
- We tested whether GABAergic signalling in an isolated forebrain preparation also showed ageing-related changes.
- A novel approach was used, whereby population imaging was coupled to quantitative pharmacological sensitivity.
- Sensitivity to $GABA_A$ blockade was inversely associated with age and cortical thickness, but hearing loss did not independently contribute to the change in $GABA_A$ergic sensitivity.
- Redox states in the auditory cortex of young and aged animals were similar, suggesting that the differences in $GABA_A$ergic sensitivity are unlikely to be due to differences in slice health.

Abstract To examine ageing-related changes in the earliest stages of auditory cortical processing, population auditory cortical responses to thalamic afferent stimulation were studied in brain slices obtained from young and aged CBA/CAj mice (up to 28 months of age). Cortical responses were measured using flavoprotein autofluorescence imaging, and ageing-related changes in inhibition were assessed by measuring the sensitivity of these responses to blockade of $GABA_A$ receptors using bath-applied SR95531. The maximum auditory cortical response to afferent stimulation was not different between young and aged animals under control conditions, but responses to afferent stimulation in aged animals showed a significantly lower sensitivity to GABA blockade with SR95531. Cortical thickness, but not hearing loss, improved the prediction of all imaging variables when combined with age, particularly sensitivity to GABA blockade for the maximum response. To determine if the observed differences between slices from young and aged animals were due to differences in slice health, the redox state in the auditory cortex was assessed by measuring the FAD+/NADH ratio using fluorescence imaging. We found that this ratio is highly sensitive to known redox stressors such as H_2O_2 and NaCN; however, no difference was found between young and aged animals. By using a new approach to quantitatively assess pharmacological sensitivity of population-level cortical responses to afferent stimulation, these data demonstrate that auditory cortical inhibition diminishes with ageing. Furthermore, these data establish a significant relationship between cortical thickness and GABAergic sensitivity, which had not previously been observed in an animal model of ageing.

DOI: 10.1113/JP271221

(Received 5 July 2015; accepted after revision 18 October 2015; first published online 27 October 2015)
Corresponding author D. Llano: 2355 Beckman Institute, 405 North Mathews Avenue, Urbana, IL 61801–2325, USA. Email: d-llano@illinois.edu

Abbreviations ABR, auditory brainstem response; AC, auditory cortex; ACSF, artificial cerebrospinal fluid; GAD, glutamic acid decarboxylase; ROI, region of interest.

Introduction

Hearing loss is the third most prevalent chronic condition in older Americans (Yueh *et al.* 2003). Despite great strides in the amelioration of ageing-related hearing loss through the use of peripheral hearing aids, older adults often continue to have substantial difficulty in real life, multi-talker, situations (Humes, 2007). These continuing difficulties may arise from a general inability to suppress distracting information found during normal cognitive ageing (Gazzaley & D'Esposito, 2007; Gazzaley *et al.* 2008; Healey *et al.* 2008). Consistent with this hypothesis is a large body of animal literature showing that synaptic inhibitory mechanisms in the auditory system are particularly vulnerable to ageing (Gutierrez *et al.* 1994; Ling *et al.* 2005; Burianova *et al.* 2009; Schmidt *et al.* 2010). In part, these changes in central inhibition may reflect a compensatory, homeostatic response to the decreased peripheral sensory input common with age (Caspary *et al.* 2008; Norena, 2011; Hébert *et al.* 2013; Gold & Bajo, 2014).

Changes in molecular and electrophysiological inhibitory properties have been found at multiple levels of the ageing auditory system. The ageing cochlear nuclei show lower glycine levels and altered glycine receptor subunit compositions (Banay-Schwartz *et al.* 1989). Functional changes include a loss of on-characteristic frequency inhibition and altered temporal responses (Caspary *et al.* 2005; Caspary *et al.* 2006). The inferior colliculus shows declines of glutamic acid decarboxylase (GAD) and GABA levels, as well as reduced levels of GABA release (Milbrandt *et al.* 1994, 2000). This decrease in inhibition may be the cause of the decreased response latencies and increased spontaneous activity seen in the aged inferior colliculi of mice (Simon *et al.* 2004; Longenecker & Galazyuk, 2011). The auditory cortex (AC) shows declines in both mRNA and protein expression of GAD, as well as changes in wild-type receptor proportions with ageing (Ling *et al.* 2005; Caspary *et al.* 2013). These changes may contribute to layer-specific increases in spontaneous activity seen disproportionately in the upper layers of primary AC and which are consistent with molecular data showing a disproportionate loss of GAD levels in the supragranular layers of rat primary AC (Ling *et al.* 2005; Hughes *et al.* 2010).

Due to the highly interconnected nature of structures at all levels of the auditory system, it is particularly difficult to know the origin of the above-described changes seen with ageing. In the AC in particular, it is unclear if the changes seen with ageing are due to the degraded peripheral hearing apparatus or due to a combination of this and resulting changes in the various nuclei that provide its input.

To isolate the effects of ageing on the thalamocortical synapse from changes in cortical responses simply related to ageing-related changes in peripheral input (Zettel *et al.* 1997; Jacobson *et al.* 2003; Sha *et al.* 2008; Parthasarathy *et al.* 2010, 2014), we have employed a brain slice preparation in which afferent fibres from the auditory thalamus are partially preserved and can be stimulated in isolation of subnuclei to produce responses in the AC (Cruikshank *et al.* 2002; Takesian *et al.* 2012). AC activation was measured using flavoprotein autofluorescence, which permits the measurement of neural activity with high sensitivity and spatial resolution, without the potentially confounding factors present when using exogenous dyes, such as differential uptake or dye toxicity (Shibuki *et al.* 2003; Llano *et al.* 2009). The stability of the flavoprotein autofluoresence signal makes it particularly suitable for exploring pharmacological differences quantitatively across experimental groups (Middleton *et al.* 2011; Llano *et al.* 2012), and thus provides a unique opportunity to explore population-level ageing-related changes in synaptic inhibition. Given the evidence for ageing-related GABAergic changes, we employed a blocker of $GABA_A$ receptors (SR95531) in our test procedures. To measure potential changes in the redox state of tissue from aged animals, as well as monitor slice health, we measured the redox ratio of the tissue at various time points during the experiment. This ratio has previously been shown to reflect tissue health (Mayevsky, 1984; Gerich *et al.* 2009; Matsubara *et al.* 2010; Sepehr *et al.* 2012; Staniszewski *et al.* 2013).

Methods

Mice

The CBA/CAj strain was used because of its gradual ageing-related hearing loss (Zheng *et al.* 1999; Ohlemiller *et al.* 2010). Due to factors such as animal death or the availability of certain data from prior data sets, the number of animals differs between different analyses and the numbers of animals used in each case are indicated in the figures and/or text. A total of 50 male mice, obtained through the National Institute on Ageing aged rodent colonies, were used in these studies, although

not all mice were used for all experiments. Several mice were lost after auditory brainstem responses (ABRs, see below) were obtained. The full, primary data set (imaging, redox ratios, hearing and cortical thickness) comprised 29 animals. Three animals were eliminated during the *post-hoc* analysis, two young and one aged, because of minor damage to the AC during the slicing procedure which affected the flavoprotein signal and one aged because of a bowel obstruction and fragile health at the time of slicing. The young group comprised 14 animals: four at 4 months, four at 5.5 months, five at 9 months and one at 13 months of age. The aged group comprised 12 animals: four at 20 months, five at 22 months, two at 23 months and one at 28.4 months. More animals were available for measures of cortical thickness. Eight animals from our previous study (Llano *et al.* 2012) without hearing threshold measurement (two at 2 months and six from 24 to 30 months) were analysed, giving 37 animals in total for this data set. All procedures were approved by the Institutional Animal Care and Use Committee at the University of Illinois. All animals were housed in animal care facilities approved by the American Association for Assessment and Accreditation of Laboratory Animal Care.

Auditory brainstem responses

ABRs were obtained at frequencies of 4, 8, 16, 32, 45 and 64 kHz as well as broadband noise. It was not possible to obtain all frequencies for all animals. Animals were anaesthetized with 100 mg kg^{-1} ketamine + 3 mg kg^{-1} xylazine intraperitoneally before the insertion of two subdermal electrodes, one at the vertex and one behind the left ear. Stimuli were presented using a Tucker-Davis (TDT) system 3 (Alachua, FL, USA), ES1 free field speaker, with waveforms being generated by RPvdsEx software. The output of the TDT speaker was calibrated at all the relevant frequencies, using a Bruel and Kjaer type 4135 microphone and a Bruel and Kjaer measuring amplifier (Model 2610; Copenhage, Denmark). Each frequency was presented for 5 ms (3 ms flat with 1 ms for both rise and fall times), at a rate of 2–6 Hz, varied within each animal, with a 100 ms analysis window. Raw potentials were obtained with a Dagan 2400A amplifier (Minneapolis, MN, USA) and preamplifier headstage combination, and filtered between 100 and 3000 Hz. An AD Instruments (Colorado Springs, CO, USA) power lab 4/30 system was used to average these waveforms 500 times. Significant deflections, assessed via visual inspection, within 10 ms after the end of the stimulus were deemed a response. All traces were reviewed by a single investigator and no attempts were made to cross-validate these thresholds. Despite this, the tone and noise threshold changes with ageing observed in this study are similar to those seen previously using this mouse strain (Ohlemiller *et al.* 2010). To keep ABR measurements within 3 months of final imaging experiments, ABRs were redone 5 months after the first set on three animals. Both sets of ABRs on those three animals at different ages were included in the ABR data set, bringing the final number of observations to 45. Thirteen of these animals either died from anaesthesia or died during housing prior to final experiments. Twenty-five of 26 of the animals in the full, primary data set had ABRs measured using noise, 8, 16 and 32 kHz, while one older animal only had a measurable response to noise and 8 kHz. Hearing threshold in response to a noise stimulus was chosen as the main hearing metric because all animals had a measurable ABR to noise and because a principal components analysis showed that noise thresholds were essentially interchangeable with virtually any combination of pure-tone thresholds or thresholds averaged across frequencies (data not shown).

Brain slicing

We modified the thalamocortical brain slice preparation developed by Cruikshank *et al.* (2002) to increase the likelihood of retaining the lateral extent of thalamocortical afferents to the left AC. To ensure maximum slice viability, mice were initially anaesthetized with ketamine (100 mg kg^{-1}) + xylazine (3 mg kg^{-1}) intraperitoneally and perfused with chilled (4°C) sucrose-based slicing solution (in mM): 234 sucrose, 11 glucose, 26 $NaHCO_3$, 2.5 KCl, 1.25 NaH_2PO_4, 10 $MgCl_2$, 0.5 $CaCl_2$. Brains were blocked by removing the olfactory bulbs and the anterior 2 mm of the frontal cortex with a razor blade. The brain was then tipped onto the coronal cut and an off-horizontal cut was made on the dorsal surface, removing a sliver of brain angled at 20 deg from the horizontal plane. This increase in cutting angle of the thalamocortical slice has also been employed previously in older gerbils (Takesian *et al.* 2012). The brain was then glued onto the cut angled surface, and 600 μm thick sections were taken. Sections were incubated for 1 h in 32°C incubation solution (mM: 26 $NaHCO_3$, 2.5 KCl, 10 glucose, 126 NaCl, 1.25 NaH_2PO_4, 3 $MgCl_2$ and 1 $CaCl_2$) before being imaged. After incubation, slices were transferred to a chamber with an elevated slice platform so that the tissue could be perfused from both above and below with artificial cerebrospinal fluid (ACSF, mM: 26 $NaHCO_3$, 2.5 KCl, 10 glucose, 126 NaCl, 1.25 NaH_2PO_4, 2 $MgCl_2$ and 2 $CaCl_2$, 22°C and bubbled with 95% oxygen/5% carbon dioxide).

Stimulation, imaging and drug application

Glass micropipettes filled with ACSF, and broken back to an external diameter of 75 μm, were used for stimulation. Whenever possible, the same electrode was used to reduce variability. Due to the considerable variability in capturing the thalamocortical afferent bundle at the level

of the thalamus (Broicher *et al.* 2010), stimulation was performed in the white matter below the AC. The electrode was lowered onto the white matter 150–200 μm ventral to the AC and 50–100 μm rostral of the hippocampus (Fig. 1*A*). Pulse trains were delivered using PowerLab software and hardware and a World Precision Instruments (Sarasota, FL, USA) stimulus isolator. Trains were 1 s in duration, with 2 ms pulses, delivered at 40 pulses per second. This train was delivered every 20 s, with five repetitions in total.

Endogenous flavoprotein (FAD+) autofluorescence was used as an indicator of neural activation (Shibuki *et al.* 2003). A stable DC fluorescence illuminator (Prior Lumen 200; Prior Scientific, Rockland, MA, USA) and a U-M49002Xl E-GFP Olympus filter cube (excitation: 470–490 nm, dichroic 505 nm, emission 515 nm long pass) were used for fluorescence optics. A coverslip was placed over the slice to minimize the effect of fluid fluctuation on imaging (Fig. 1*B*). All data were collected at 4 frames per second using an infinity-corrected Olympus MacroXL 4× objective (NA 0.28) and a Retiga EXi camera using 4 × 4 binning and StreamPix software. NADH imaging was performed using a Semrock Sirius A 000 cube with 350–390 nm excitation and 415–465 nm emission. Redox ratios were expressed as a ratio of FAD+ to NADH (Sepehr *et al.* 2012).

The concentration of SR95531 (6-imino-3-(4-methoxyphenyl)-1(6H)-pyridazinebutanoic acid hydrobromide; Tocris, Ellisville, MO, USA) was 150 nM, which is slightly higher than estimates of the synaptic IC_{50} for SR95531 (Lindquist *et al.* 2005). In all cases, SR95531 was dissolved in ACSF just prior to the experiment. After washing in SR95531 in ACSF for 1 h, several stimuli were applied to the fibre bundle to assess for stability of the AC response. Once stability was observed, experiments were started (typically producing a total wash-in time of 1.5 h).

Analysis

For each run, a total of 420 images, binned 4 × 4 to a final size of 260 × 348 pixels, were collected. The first 5 s (20 frames) functioned as a baseline for the subsequent images. All image analysis was done using custom software written in MATLAB (The Mathworks, Inc., Natick, MA, USA). Time-based analyses were done by computing the change in fluorescence as a function of baseline fluorescence (Fig. 1*C*). Time series for each pixel

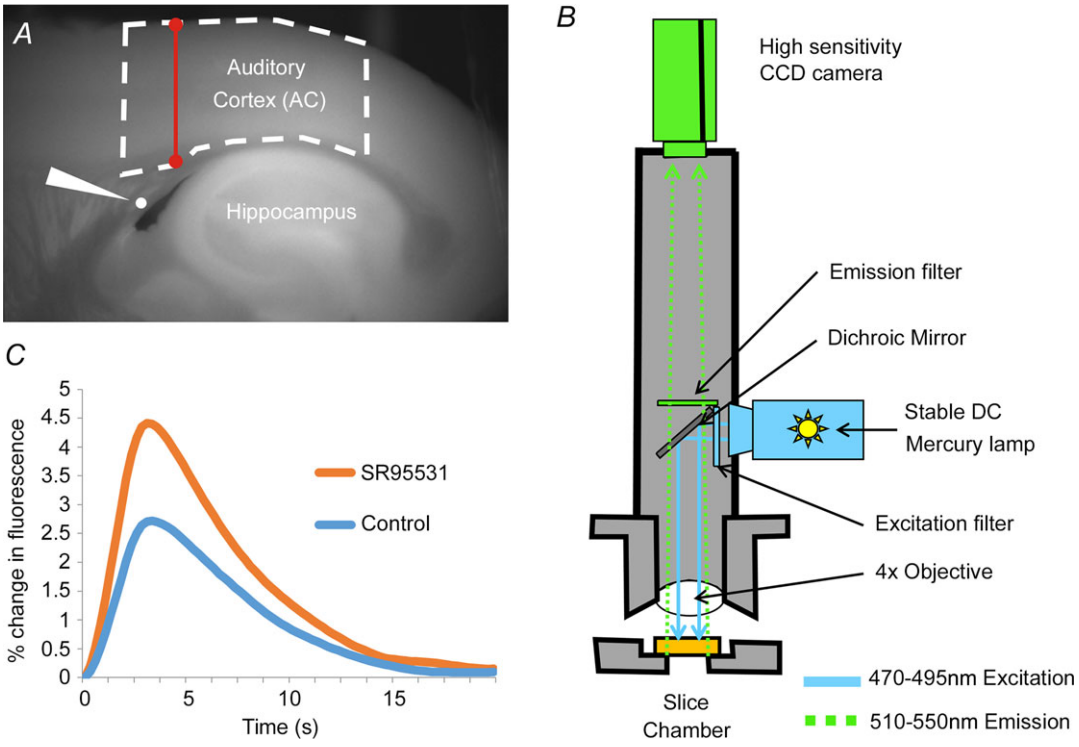

Figure 1. Experimental set-up
A, raw FAD+ of a brain slice as it sits in the chamber, illustrating the position of the AC, the stimulating electrode (white wedge) and the hippocampus. Dashed line represents the ROI analysed. Red barbell represents the location where cortical thickness was measured. *B*, schematic diagram of the imaging rig, illustrating the wavelengths for excitation and emission, positions of the light source and camera, as well as the associated optics. *C*, time course of FAD+ signal, both under control conditions and in the presence of SR95531, illustrating the relatively slow rise and fall of the FAD+ signal.

were corrected for quenching by high-pass filtering each time series using a high-frequency cutoff of 0.025 Hz. A series of stimulation amplitudes were used, ranging from 5 to 450 μA, and an input–output curve was constructed. Input–output curves generally resembled a sigmoidal function, and therefore a traditional, four-parameter dose–response curve was fit using a custom program in SAS (SAS Institute Inc., Cary, NC, USA). Note that in some cases the slope of the input–output function appeared shallower at low amplitudes (see e.g. Fig. 4), particularly in older animals. Nevertheless, we continued to use a four-parameter model, rather than a higher order model, to avoid overfitting. In addition, by using this model, we, if anything, underestimated the leftward shift of the input–output function that is described in the Results section.

From the fit curves, the minimum, maximum, mid-point (EC_{50}) and slope could be extracted (see Fig. 3*I*). Each of these parameters probably reflects a different underlying biological process. For example, the maximal response is probably a reflection of the total amount of synaptic input to a particular region of interest (Llano *et al.* 2009), while the slope may reflect the ability to recruit axons of different diameters as stimulation strength is increased (Kiernan *et al.* 2001). Although absolute threshold was not measured here, EC_{50} is a comparable metric and is probably related to underlying excitability of the stimulated axons (Kiernan *et al.* 2001). Outliers, specifically at the highest stimulation amplitudes, can have a large effect on the curves. Outliers are produced as a result of several experimental factors, such as random fluctuations in flow rates in the chamber, or due to order effects from stimulation (which is why ordering of stimulus amplitudes was randomized). We eliminated these outliers by first fitting the curves, then taking the residuals and discarding any point with a residual more than 2 standard deviations from the mean. The process was repeated until no outliers were detected. As a result of this process, 2.87% (17 of 593) of the data points were removed as outliers. These parameters in the different conditions (control ACSF, SR95531 and ratio of response under SR95531 to control ACSF conditions) were then analysed as dependent variables.

Our primary region of interest (ROI) contains primary auditory fields and was generated using a combination of activation data and anatomical data. The activation area in our slices (see Fig. 3*A*–*H*) overlaps with parvalbumin staining in the thalamocortical slice used to distinguish primary auditory fields from non-primary (Llano *et al.* 2012), with the area identified as receiving topographic projections being the ventral division of the medial geniculate body (Hackett *et al.* 2011) and also seen to be activated after inferior colliculus stimulation in the colliculo-thalamocortical slice (Llano *et al.* 2014). However, we do not attempt to distinguish the primary auditory fields (primary AC and/or anterior auditory field) and therefore refer to this region more generally as AC. The rostral-most extent of the ROI was defined by drawing a line from the subcortical white matter to the pia along the rostral edge of the columnar flavoprotein activation profile without $GABA_A$ blockade. This line was then extended along 2 mm of cortex in the caudal direction (Cruikshank *et al.* 2002; Hackett *et al.* 2011).

The AC ROI was also used to evaluate the ratio of FAD+ fluorescence to NADH fluorescence (redox ratio) over the course of the experiment as a surrogate marker for tissue health. At several time points throughout the experiment, several frames of baseline FAD+ and NADH fluorescence were taken sequentially. These frames were obtained in between stimulus runs. Of these, three frames were averaged and the ROI for the AC was used to find the average pixel intensity in the composite image. The average intensities were then divided to yield the final ratio. This ratio was compared between young and old animals at 12 time points during the experiment. To measure the sensitivity of this redox ratio to oxidative stress, we exposed a slice to three increasing concentrations of H_2O_2 and two increasing concentrations of NaCN to show both dose-dependent increases and decreases in the ratio, respectively. Cortical thickness was evaluated by drawing a line tangent to the rostral-most extent of the hippocampus, from the white/grey matter border of the cortex to the pia (see Fig. 1*A* for an illustration of where cortical thickness was measured).

Statistics

Given the relatively small numbers of animals in each group, non-parametric statistics were used for most group-wise comparisons. Given the non-uniform distribution of ages in the study (mostly young or aged animals, with few in between), pairwise comparison was done for most analyses. All pairwise comparisons used a two-tailed Wilcoxon rank sum test. All P values and correlation coefficients reported for correlations are Spearman correlations. For measurement of the impact of age on cortical thickness, linear regression with a 95% confidence interval was performed to extract variables of interest such as the slope of cortical thickness decline with age indicating the mean decline per year. Multiple linear regression was used to test relative contributions of age, hearing loss and cortical thickness. Age, hearing and cortical thickness were included as independent variables and the adjusted R^2 values for their inclusion were compared. To evaluate whether FAD+/NADH ratios were different at any point during the experiment, we employed a repeated-measures ANOVA assuming mixed effects. All statistical analysis was generated using SAS software, Version 9.4 of the SAS System for Windows.

Results

Hearing

Consistent with previous work, CBA/CAj mice show V-shaped ABR threshold curves with greatest sensitivity around 16 kHz, and an increase in threshold with ageing (Fig. 2*A*) (Zheng *et al.* 1999). The increase in threshold was similar across all frequencies tested. The young animals in our experiments had a mean threshold to hearing threshold stimulation of 27.4 dB SPL (SD 4.9) while the aged animals had a mean threshold of 46.4 dB SPL (SD 19.7, $P<0.0001$, Fig. 2*B*).

AC activation differences

The input–output functions in both control ACSF (Fig. 3*A–D*) and SR95531 (Fig. 3*E–H*) resembled a sigmoidal function (Fig. 3*I*) in both young and aged animals. Qualitative comparison of the averaged input–output functions of young *versus* old animals under control and SR95531 conditions suggests that these curves have different shapes. Under control conditions, the input–output curves for aged animals appear to have a lower EC_{50} and shallower slope than young animals (Fig. 4). Exposure to SR95531 shifts both curves upward and to the left, although the degree of upward shift appears less pronounced in aged animals, suggesting diminished sensitivity to $GABA_A$ blockade with ageing. These trends are quantitatively compared below.

The maximum activation in the control condition did not differ between old and young animals (Fig. 5*A*). In the control ACSF condition, the mean AC response for young animals was 6.04% (SD 1.58, $n = 14$) above baseline and 5.29% (SD 1.23, $n = 12$) for aged animals; the difference was not significant ($P = 0.25$). However, the third quartile and maximum were higher in young animals (7.24%and 8.53% for young *vs.* 6.33 and 6.54% for aged). Thus, for the young mice the upper range of the maximum peak under control conditions extends beyond that in the aged mice. In the presence of SR95531, there was significantly greater activation in the AC of young animals than in older animals (8.7% (SD 1.87, $n = 14$) *vs.* 6.12% (SD 1.52, $n = 12$), $P = 0.003$, Fig. 5*B*). As we have done previously (Llano *et al.* 2012), the ratio of the response to stimulation under SR95531 to the response under control conditions was used as an indicator of the sensitivity of the AC to $GABA_A$ blockade. This was done to mitigate baseline differences across animals. This ratio was about 30% higher (Fig. 5*C*; $P = 0.004$) in the young animals (1.51 (SD 0.32, $n = 12$)) than in the aged (1.16 (SD 0.18, $n = 14$)), suggesting a greater sensitivity to $GABA_A$ergic blockade in young animals.

Two other parameters of the fitted sigmoid curve (EC_{50} and slope) were examined similarly, with the hypothesis that ageing-related changes in cortical GABAergic function may either shift this function laterally (EC_{50}) or change the recruitment pattern of thalamocortical putative afferents (slope). The mean EC_{50} in the control ACSF condition was significantly higher in younger animals (130.5 μA (SD 32.7, $n = 14$)) than for aged animals (91.3μA (SD 39.4, $n = 12$, Fig. 6*A*; $P = 0.008$)). EC_{50} differences also remained significant ($P = 0.01$) with an aged mean of 63.0 μA (SD 33.4) and a young mean of 103.9 μA (SD 33.04) under conditions of $GABA_A$ blockade (Fig. 6*B*), although the ratio of these was not different ($P = 0.121$), and had nearly completely

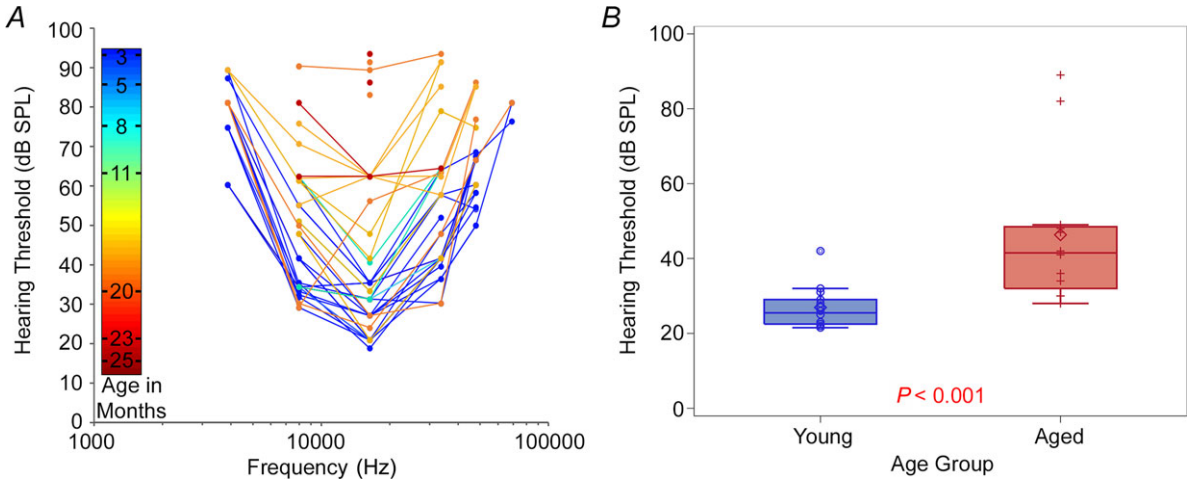

Figure 2. Hearing thresholds
A, changes in hearing threshold, as measured using ABRs in response pure tones at frequencies of 4–64 kHz, as a function of age. The colour bar corresponds to age of animal in months. *B*, mean hearing threshold, measured using ABRs in response to broadband noise, in young *versus* aged animals.

overlapping distributions (Fig. 6*C*), suggesting similar sensitivities of EC_{50} to $GABA_A$ blockade in young and aged animals. To approximate the threshold for responding to a weak stimulus, the EC_{10} was computed from the fitted input–output curves. The EC_{10} was also smaller in aged animals than younger animals (41.0 μA (SD 29.6), $n = 12$, *vs.* 71.1 μA (SD 29.2), $n = 14$; $P = 0.014$), suggesting a greater sensitivity to weak signals in older animals.

We also compared the slope in the control ACSF condition, for which the young mean was 3.57×10^{-2} % μA^{-1} (SD 0.84, $n = 14$) and the aged mean was 2.26×10^{-2} % μA^{-1} (SD 0.60, $n = 12$), and found that older animals have a shallower slope in the control condition (Fig. 6*D*; $P = 0.001$). Exposure to SR95531 caused both slopes to increase, such that the slopes were no longer significantly different ($P = 0.350$, Fig. 6*E*), and that their sensitivities to $GABA_A$ blockade were similar because their ratios were not significantly different ($P = 0.463$, Fig. 6*F*).

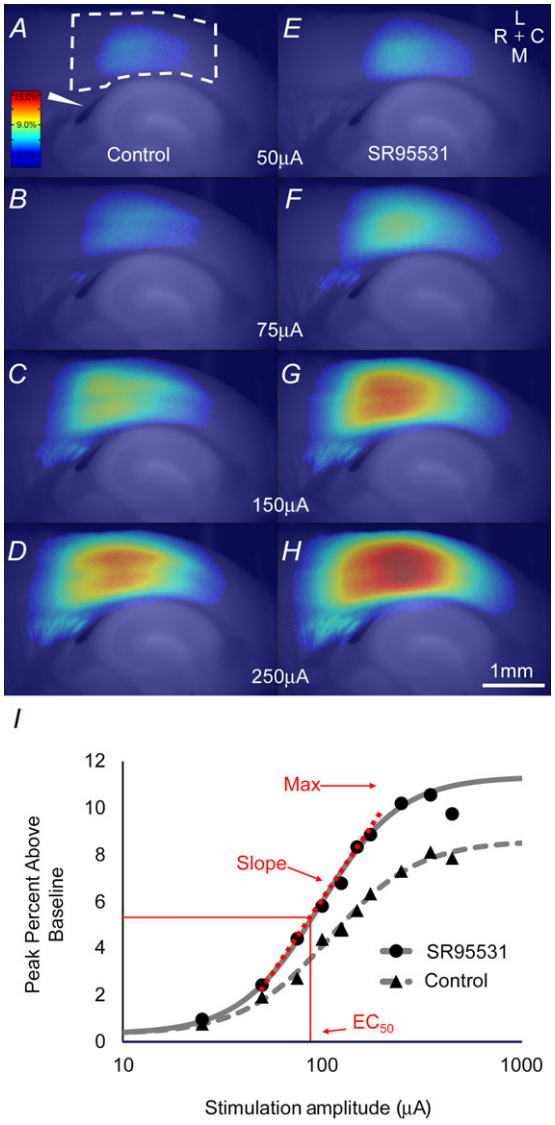

Figure 3.
A, activation in the AC of a young animal in response to electrical stimulation of white matter at 50 μA. The colour bar shows colours corresponding to the maximum percentage above baseline generated by the flavoprotein signal. The wedge indicates the stimulating electrode location. Dashed line represents the AC ROI. Scale bar in *H* is 1 mm. *B–D*, progressively increasing amplitudes of stimulation in control ACSF. *E*, activation in SR95531 conditions to 50 μA. The compass rose indicates: medial (M), lateral (L), rostral (R) and caudal (C). *F–H*, progressively increasing amplitudes of stimulation in SR95531 ACSF. *I*, sigmoid curves fit to all data points from this animal in both the control ACSF condition and SR95531 condition. Red lettering and arrows show the locations for maximum and EC_{50} for the SR95531 curve, as well as the portion of the curve where the slope was derived. Activation shown here is relatively high, but representative of the data seen in this study.

Table 1. *P*-values for Spearman correlations between age, hearing threshold and cortical thickness using the ratio of SR95531 to control (sensitivity) for maximum activation, EC_{50} and slope as dependent variables ($n = 26$ for all comparisons)

Variables	Age	Hearing threshold	Cortical thickness
Maximum activation	0.025	0.072	<0.001
EC_{50}	0.364	0.086	0.911
Slope	0.069	0.241	0.831

Impact of cortical thickness and hearing loss

Cortical thickness was measured in the rostral margin of the AC, and animals were included in this analysis from a previous study (Llano *et al.* 2012), which were imaged in the same way as the current study. Decline of cortical thickness with age was found to be linear with a slope of -0.073 mm year^{-1} ($R^2 = 0.60$, $P < 0.0001$, $n = 37$; Fig. 7). Given the relationship between ageing and hearing loss (Fig. 2) and cortical thickness (Fig. 7), we examined the strength of the association between age (in months), cortical thickness (in mm) or hearing loss (in dB SPL) with sensitivity to SR95531 for maximum, EC_{50} and slope (Table 1). We found that the best predictor of sensitivity to $GABA_A$ergic blockade for the maximum response was cortical thickness ($P < 0.001$, $R^2 = 0.469$, $n = 26$, Spearman's correlation). Note the borderline *P*-values for hearing threshold when correlated to maximum activation and EC_{50}. Given the modest correlations between hearing threshold and these two variables (Spearman's rho = 0.361 and 0.340, respectively), our study had a power of approximately 60% power of detecting statistical significance with an alpha value of 0.05. This finding suggests that at a sample size of 28, we cannot exclude the possibility that there is

a significant correlation between hearing threshold and these two variables.

A multiple regression model was used to assess the impact of combinations of independent variables on the sensitivity to $GABA_A$ergic blockade on the maximum response. Inclusion of hearing loss or cortical thickness in the model containing age revealed that only cortical thickness increased the performance of the model. Inclusion of hearing loss had no additional impact on the ability to predict changes in sensitivity to $GABA_A$ergic blockade (baseline adjusted $R^2 = 0.184$ with only age as a predictor, adjusted $R^2 = 0.150$ with hearing loss + age, adjusted $R^2 = 0.227$ with cortical thickness + age). For EC_{50} and slope, similar to age, neither hearing loss nor cortical thickness served as a significant predictor of sensitivity (ratio) to $GABA_A$ergic blockade (Table 1). Additionally, for all non-sensitivity/ratio-dependent variables (maxima, EC_{50}, slope), in both conditions (control and SR95531), models with cortical thickness and age were in all cases superior (higher adjusted R^2 values) to those with age alone and those with age and hearing (data not shown).

Redox ratios

As a way to test for potential differences in the health of slices taken from young *versus* aged animals, redox ratios were measured both at baseline and over the course of the experiment to monitor slice health (Fig. 8*A*). The use of redox ratios is based on findings that redox ratio is correlated to tissue health across several different tissue types including the brain (Mayevsky, 1984; Gerich *et al.* 2009; Matsubara *et al.* 2010; Sepehr *et al.* 2012; Staniszewski *et al.* 2013). During the course of the experiment, the redox ratios do tend generally to decline (repeated measures ANOVA, $P < 0.0001$), although there were no differences between young and aged (Fig. 8, $P = 0.139$). Note that there are fluctuations in the

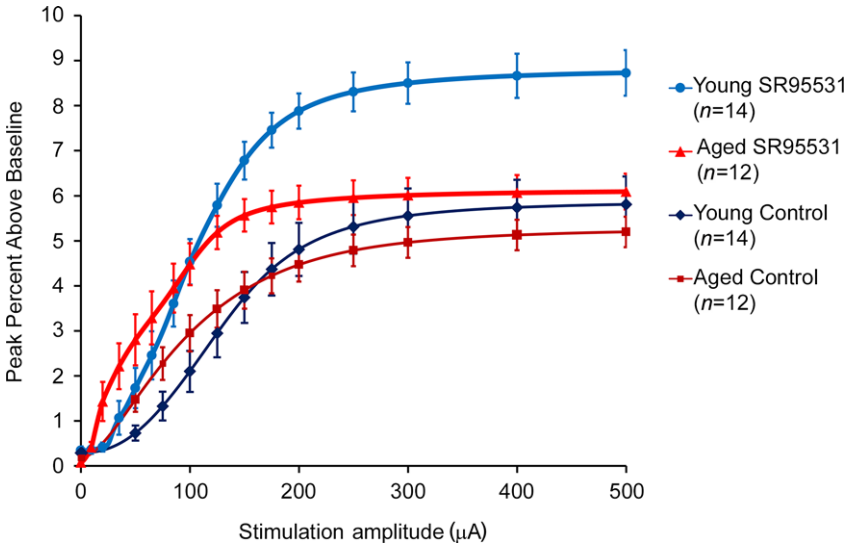

Figure 4. Averaged input–output curves from young and aged animals in control and SR95531 conditions
Values are displayed as mean and SEM at standard stimulation amplitudes. Data to compute the means are derived from the fitted sigmoidal input–output curves.

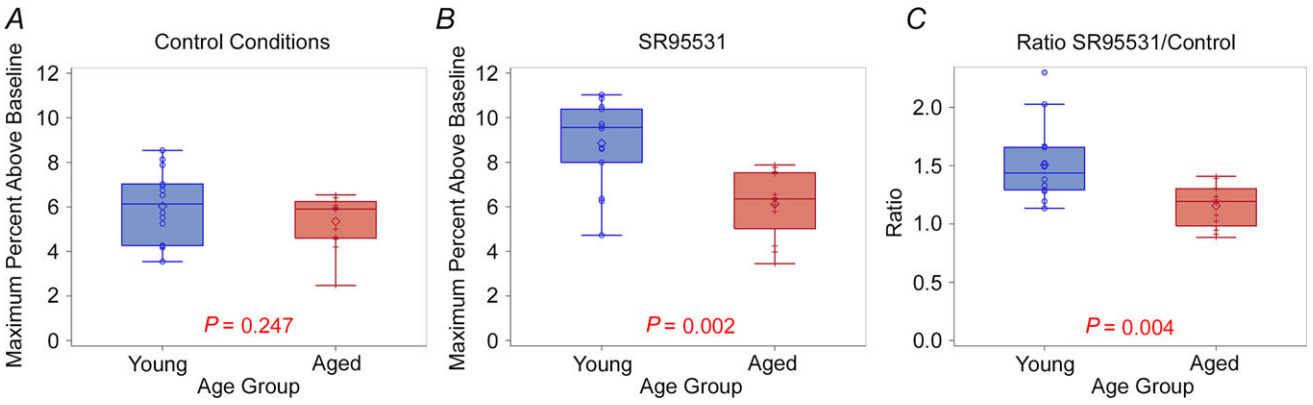

Figure 5. Maximum activation for young and aged animals
A and *B*, pairwise comparisons of the maximum activation for young and aged animals under control conditions (*A*) and in the presence of SR95531 (*B*). *C*, pairwise comparison of the ratio of the maximum response under SR95531 conditions to control conditions in young *versus* aged animals.

redox ratio that correspond to different experimental conditions. When redox ratio was assessed in between electrical stimulation runs under control conditions, there was a gradual drop in the ratio. During the SR95531 wash-in (and when no stimulation was occurring), the ratio appeared to recover. When stimulated again, now under conditions of SR95531 exposure, the ratio again dropped, and recovered during the SR95531 washout, again when no stimulation was occurring. As redox ratio has not yet been established as a measurement of auditory cortex slice health, the sensitivity of redox ratio measurements to substances known to be metabolic stressors was also assessed (Fig. 9). The administration of three increasing concentrations of H_2O_2 (0.1, 1 and 10 mM), bath-applied to a slice from a young animal, showed a dose-dependent increase in redox ratio. The addition of two concentrations of NaCN showed dose-dependent decreases in the redox ratio; washes returned the tissue to baseline values. These changes were similar in all regions of the slice. An ROI from off the slice in the image showed only minor fluctuations, probably as a result of reflectance of light from the neighbouring tissue.

Discussion

Summary

In this study, we observed that aged CBA/CAj mice demonstrate changes in auditory cortical responses to putative afferent stimulation when compared to young controls. Without $GABA_A$ergic blockade, the maximum strengths of activation were not different between young and aged brains. However, differences were seen when the tissues were exposed to a low concentration of SR95531; the maximum responses in aged animals showed diminished sensitivity to $GABA_A$ergic blockade. The EC_{50} and slope of the input–output curves were both lower in older animals. Hearing loss and cortical thickness were strongly correlated with age, and cortical thickness was a better predictor of $GABA_A$ blockade sensitivity for the maximum response than either age or hearing loss. Finally, no significant differences were seen in the redox ratio between slices obtained from young and aged animals. These data suggest ageing in mice is associated with hearing loss, decreases in AC thickness and diminished sensitivity to $GABA_A$ergic inhibition, and that the differences noted in the current study are unlikely

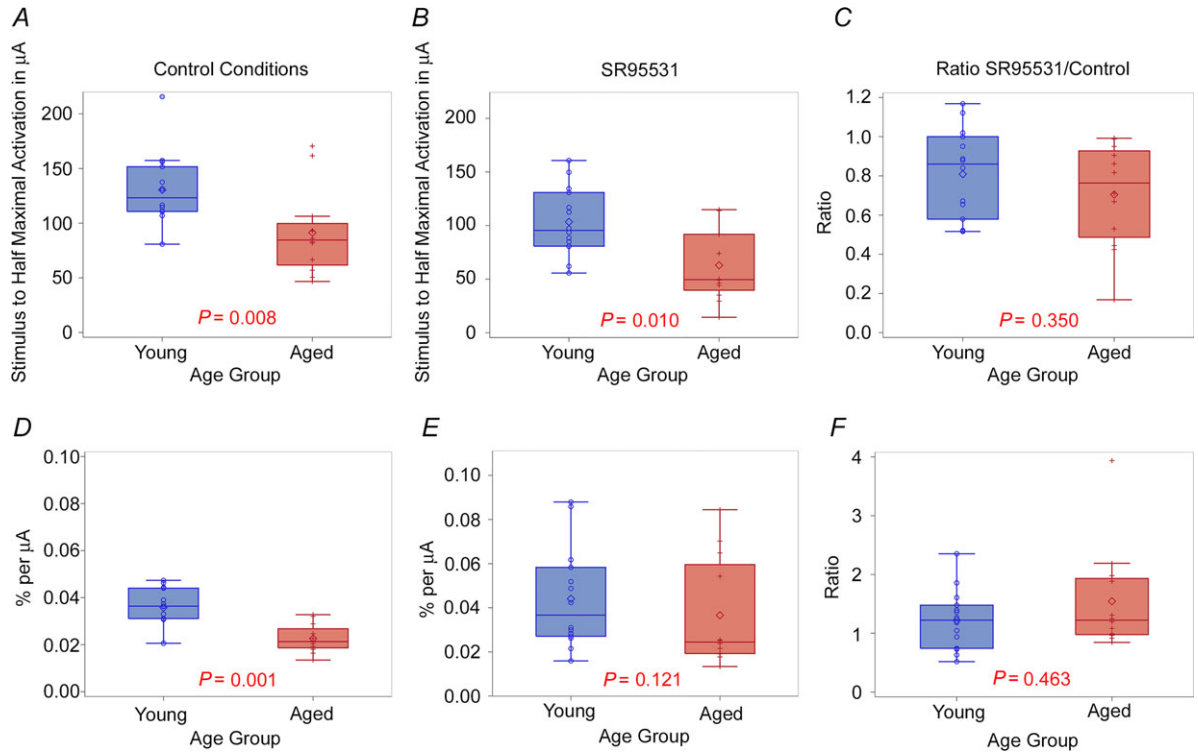

Figure 6. EC_{50} and slope of the input–output functions for young and aged animals
A and *B*, pairwise comparisons of the EC_{50} for young and aged animals under control conditions (*A*) and in the presence of SR95531 (*B*). *C*, pairwise comparison of the ratio of the EC_{50} under SR95531 conditions to control conditions in young *versus* aged animals. *D* and *E*, pairwise comparisons of the slope of the input–output functions for young and aged animals under control conditions (*D*) and in the presence of SR95531. *F*, pairwise comparison of the ratio of the slope under SR95531 conditions to control conditions in young *versus* aged animals.

to be a reflection of tissue health between slices from young and aged animals.

Methodological considerations

One relevant concern is the tissue health of aged slices at 600 μm. This thickness was used to retain maximal connectivity within the slice. Other groups have had success with such slices at this thickness (Cruikshank *et al.* 2002; Chang *et al.* 2005; Luebke & Chang, 2007) and studies using even thicker slices suggest that in slices from young animals central necrosis begins at 800–900 μm (Llano *et al.* 2014). Although many studies examining slices from aged animals demonstrate changes compared to young animals in terms of synaptic properties (Luebke *et al.* 2004; Richardson *et al.* 2013), several studies examined parameters of cellular health from aged slices and generally found no difference in resting membrane potential or input resistance (Segal, 1982; Taylor & Griffith, 1993) or spike size, spike overshoot, after-potential and excitatory postsynaptic potentials (Segal, 1982). In the current experiments, additional precautions were taken to maximize the health of the slices, including perfusing with high-sucrose cutting solution (Aghajanian & Rasmussen, 1989), and using a double-perfusion slice chamber, as we have described previously (Llano *et al.* 2014). We also observed no difference in redox ratio, a surrogate marker of tissue health, between slices from young and aged animals. Although redox ratio has not, to our knowledge, been used previously to assess tissue health in the auditory cortex in brain slices, it has been used for this purpose both inside and outside the nervous system (Mayevsky, 1984; Matsubara *et al.* 2010; Sepehr *et al.* 2012; Staniszewski *et al.* 2013). We also determined that redox ratio is a sensitive marker of tissue oxidative stress, as low concentrations of H_2O_2 and NaCN induce dose-dependent changes in redox signal, as seen previously (Gerich *et al.* 2009). In addition, the redox signal does change over the course of the experiment, as shown in Fig. 8*B*, and there are fluctuations in redox ratio that correlate with parts of the experiment that presumably cause the most metabolic stress in the tissue (i.e. the portions of the experiment during which electrical stimulation was occurring). The expected direction of change of the redox ratio in these studies has not yet been established. With two different types of oxidative stress (H_2O_2 and NaCN), the ratio changed in different directions (Fig. 9), and similar discrepancies have been seen previously with the flavoprotein signal in response to low glucose (increase in signal) *versus* low oxygen (decrease in signal) (Shibuki *et al.* 2003; Gerich *et al.* 2009). It is certainly possible that ageing produces offsetting changes in the redox ratio, such that there were significant differences in tissue health that were masked by offsetting directions of the redox ratio. However, in these experiments, the patterns of the change in redox ratio between the two populations were virtually identical (Fig. 8*B*), suggesting similar sensitivities to metabolic stressors.

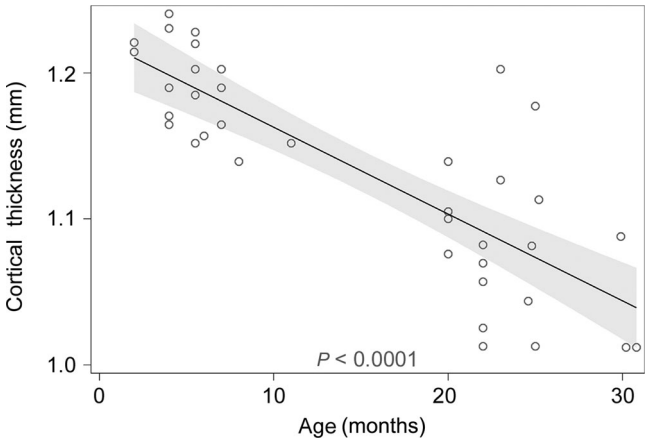

Figure 7. Cortical thickness in the AC declines linearly with age
The shaded region corresponds to 95% the confidence interval surrounding the regression line. Note the greater variability in the aged animals.

Another methodological concern is the use of similar-sized ROIs, despite the thinning of the cortex with age. No attempt was made to compensate for the thinning of the cortex, so the ROIs in the aged animals are slightly smaller in area than the young animals. We have, in fact, used several permutations of the ROI, both larger and smaller, and found similar ageing-related changes as described in our main findings (data not shown). Given this, and the fact that the majority of the flavoprotein signal was found near the centre of the ROI, it is unlikely that small differences in ROI area caused any impact in our comparison of young *versus* aged animals.

A final methodological consideration in the current work is use of electrical stimulation of a white matter path to activate the AC. It is certainly possible that electrical stimulation drives antidromic responses in the AC and that changes in SR95531 sensitivity are related to GABAergic synapses driven by branches of antidromically activated corticofugal neurons. Note, however, that in an identical experimental preparation, we determined that approximately 80% of the signal in the AC disappeared with AMPA and NMDA blockade, suggesting the most of the flavoprotein signal is generated by orthodromic activation (Llano *et al.* 2012). This finding suggests that most of the flavoprotein signal analysed in this study is generated by the thalamocortical afferents to the cortex. Nevertheless, it is possible that antidromic activation could (through local collaterals) contribute to the flavoprotein signal and the differential responses seen in young *versus* aged animals.

Ageing effects and synaptic mechanisms

The main finding of the current study is that ageing is associated with a diminished sensitivity to SR95531 in the aged AC. This is consistent with several other studies demonstrating a loss of GABAergic inhibition in the AC and other central auditory structures with ageing (Gutierrez *et al.* 1994; Ling *et al.* 2005; Burianova *et al.* 2009; Schmidt *et al.* 2010; Caspary *et al.* 2013). Similar declines in inhibition as those seen here could result largely from hearing loss rather than ageing alone (Kotak *et al.* 2005; Takesian *et al.* 2009), and interactions may occur such that ageing may exacerbate insult-induced hearing loss (Miller *et al.* 1997). Future studies employing a hearing loss paradigm in younger animals may help to separate the influences of ageing *versus* peripheral hearing loss.

An alternative explanation for our finding that aged tissue is less sensitive to $GABA_A$ergic inhibition is that SR95531 bound less effectively to its receptor in aged animals, due to, for example, changes in subunit composition of the $GABA_A$ receptor. The $GABA_A$ receptor subunit composition changes continually with age and relative changes of component subunits are brain region specific (Yu *et al.* 2006; Caspary *et al.* 2013). Complicating this interpretation is that the SR95531-related ageing

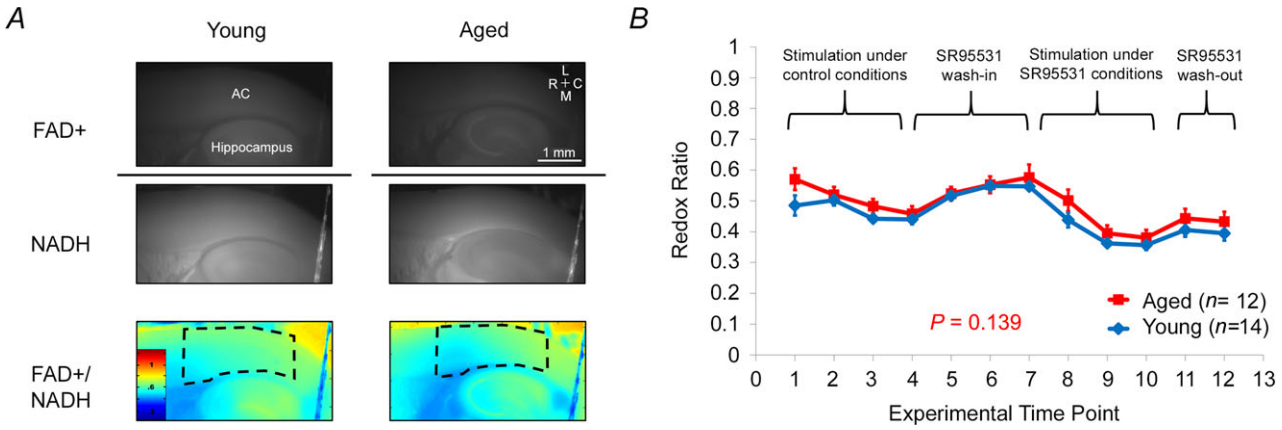

Figure 8.
A, raw images of FAD+ signal (top) and NADH signal (bottom) from an example young and old animal. The ratio of these images (hence the dividing line) is shown below as a heatmap. Scale bar = 1 mm. Dashed lines represent AC ROIs. *B*, the redox ratio (FAD+/NADH) in the AC at experimentally relevant time points. Ratio 1, before stimulation; 2, after test stimulations and immediately before series of control stimulations; 3, 50% through stimulations in control ACSF; 4, immediately following conclusion of control stimulations; 5, 10 min after SR95531 washin; 6, 30 min after SR95531 washin; 7, 1.5 h immediately preceding SR95531 stimulations; 8, 50% through SR95531 stimulations; 9, immediately following SR95531 stimulations; 10, washout of SR95531, 10 min; 11, washout of SR95531, 30 min.

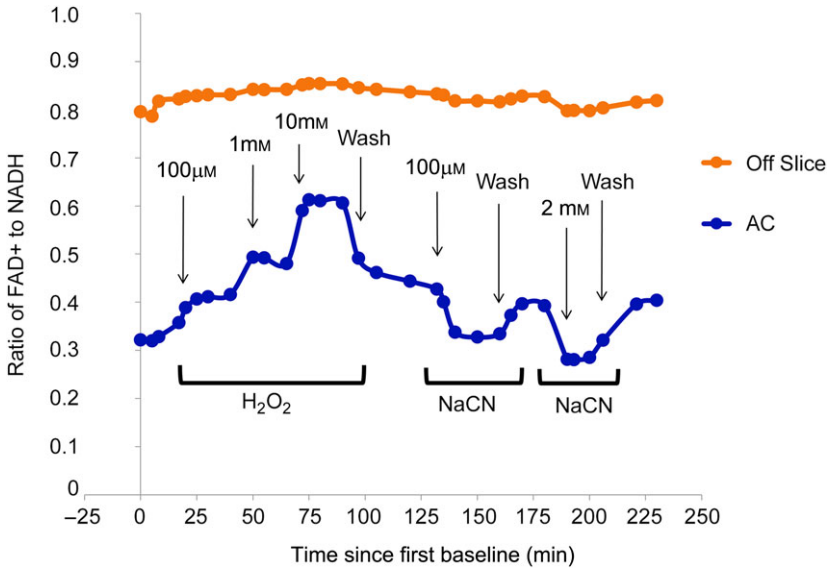

Figure 9. Redox ratio in the slice as perturbed by three increasing concentrations of H_2O_2 and two concentrations of NaCN
Three measurements established a baseline and washouts were performed after the highest concentration of H_2O_2, between the two concentrations of NaCN and at the end of the experiment to determine the new baseline.

effects in this study were not uniform across the three imaging variables studied (maximum increase in fluorescence, EC_{50} and slope). As described in the Methods, it is likely that these imaging variables provide different information about the cortical response, thus leading to differential sensitivity to $GABA_A$ergic blockade. The mixed impact of $GABA_A$ergic blockade may also be related to heterogeneity in SR95531's effects. SR95531 is considered a competitive antagonist at the GABA site on $GABA_A$ receptors, and may also function as an inverse agonist and negative allosteric modulator of GABA receptors (Ueno *et al.* 1997). Other studies suggest that SR95531 and GABA may bind to different sites (Lindquist *et al.* 2005). Therefore, the ageing-related changes in SR95531 effects seen here may be related to down-regulation of the $GABA_A$ receptor and/or changes in subunit composition.

Other neurotransmitter changes in ageing may also contribute to the current findings. In a previous study using a virtually identical preparation, we showed that approximately 20% of the flavoprotein autofluoresence signal in aged animals in the AC disappeared in the presence of APV, suggesting that there is a significant NMDA component to this signal (Llano *et al.* 2012). Given the known drop in cortical NMDA receptor density and changes in subunit composition that occur with ageing (Hof *et al.* 2002; Bai *et al.* 2004; Magnusson, 2012), it is possible that the AC signal in aged animals contains a larger proportion of non-NMDA signal than young animals. This could potentially contribute to baseline differences seen between young and aged animals observed in this study, such as EC_{50} differences, or to the differences seen when exposed to SR95531, due to repetitive activity. This will have to be examined in future work.

Fibre recruitment

We observed a difference in the shapes of input–output functions from young and aged animals, which opens the possibility that axonal fibre recruitment, excitability or myelination differences may distinguish tissue from young and aged animals. Previous studies in the peripheral nervous system, using simulation paradigms similar to ours, also report ageing-related increases in threshold and decreases in slope (Kiernan *et al.* 2001; Jankelowitz *et al.* 2007). Although absolute threshold was not measured here, EC_{10} is a comparable metric and was found to be consistently lower in older animals rather than higher in the aforementioned studies. In this study, a decline in the slope of the input–output function with ageing was observed. In the peripheral nervous system, similar changes in slope are thought to reflect differences in the distribution of axon diameters (Kiernan *et al.* 2001). Supporting this idea, there is evidence for axonal damage and demyelination *in vivo* in the AC of ageing humans with presbycusis, via decreases in *N*-acetylaspartate + *N*-acetylaspartylglutamate (Profant *et al.* 2013). Therefore, our observed ageing-related declines in slope in the control condition may have to do with ageing-related widening of the distribution of axon fibres and their subsequent recruitment. Both loss of small (Chase *et al.* 1992) and large diameter axons (Fortune *et al.* 2014), in isolation, have been seen with ageing. One potential implication of the leftward shift of the input–output functions is that the ageing AC may actually have an increased sensitivity to weak signals emanating from the thalamus, which may correlate with the known sensitivity to weak or distracting sounds that occurs in presbycusis (Tun *et al.* 2002; Helfer & Freyman, 2008).

We also observed ageing-related decreases in cortical thickness, which has also been described in humans across multiple studies (Sowell *et al.* 2003; Salat *et al.* 2004; Thambisetty *et al.* 2010) as well as rats (Ouda *et al.* 2003). The rate of decline in the current study (approximately 73 μm year^{-1}) is less than that described in rats (approximately 200 μm year^{-1}), where cortical thickness was estimated after tissue processing and, presumably, shrinkage occurred. Note that shrinkage may differ in young and old brains (Haug *et al.* 1983). In the current study, the tissue was not processed prior to measuring thickness and may represent a more accurate measurement of thickness. Interestingly, in the current study cortical thickness, which in humans correlates strongly with host cognitive functions (Milad *et al.* 2005; Choi *et al.* 2008; Dickerson *et al.* 2008), correlated more strongly to $GABA_A$ blockade sensitivity of the maximal activation than did either chronological age or hearing threshold (Table 1). These data suggest that cortical thickness may be a more appropriate biological mediator of the ageing process and that the highly variable phenotypes often seen with ageing may be explained, in part, by cortical thickness. In addition, because ageing-related decreases in cortical thickness are not thought to be related to loss of neurons, and are more probably due to decreases in synaptic density (Haug *et al.* 1983; Terry *et al.* 1987; Masliah *et al.* 1993; Dumitriu *et al.* 2010), our data suggest that ageing is associated not with loss of GABAergic neurons in the AC, but rather loss of GABAergic synaptic density or synaptic transmission.

Conclusions

The current findings add to the growing literature demonstrating that presbycusis is associated with disrupted inhibition in the central auditory system. The use of a brain slice establishes that at least part of the previously described ageing-related changes in AC are local. Additional work will be needed to separate the impact of hearing loss from ageing effects on the changes observed in this study.

References

Aghajanian GK & Rasmussen K (1989). Intracellular studies in the facial nucleus illustrating a simple new method for obtaining viable motoneurons in adult rat brain slices. *Synapse* **3**, 331–338.

Bai L, Hof PR, Standaert DG, Xing Y, Nelson SE, Young AB & Magnusson KR (2004). Changes in the expression of the NR2B subunit during aging in macaque monkeys. *Neurobiol Aging* **25**, 201–208.

Banay-Schwartz M, Lajtha A & Palkovits M (1989). Changes with aging in the levels of amino acids in rat CNS structural elements. II. Taurine and small neutral amino acids. *Neurochem Res* **14**, 563–570.

Broicher T, Bidmon HJ, Kamuf B, Coulon P, Gorji A, Pape HC, Speckmann EJ & Budde T (2010). Thalamic afferent activation of supragranular layers in auditory cortex in vitro: a voltage sensitive dye study. *Neuroscience* **165**, 371–385.

Burianova J, Ouda L, Profant O & Syka J (2009). Age-related changes in GAD levels in the central auditory system of the rat. *Exp Gerontol* **44**, 161–169.

Caspary DM, Hughes LF & Ling LL (2013). Age-related $GABA_A$ receptor changes in rat auditory cortex. *Neurobiol Aging* **34**, 1486–1496.

Caspary DM, Hughes LF, Schatteman TA & Turner JG (2006). Age-related changes in the response properties of cartwheel cells in rat dorsal cochlear nucleus. *Hear Res* **216–217**, 207–215.

Caspary DM, Ling L, Turner JG & Hughes LF (2008). Inhibitory neurotransmission, plasticity and aging in the mammalian central auditory system. *J Exp Biol* **211**, 1781–1791.

Caspary DM, Schatteman TA & Hughes LF (2005). Age-related changes in the inhibitory response properties of dorsal cochlear nucleus output neurons: role of inhibitory inputs. *J Neurosci* **25**, 10952–10959.

Chang YM, Rosene DL, Killiany RJ, Mangiamele LA & Luebke JI (2005). Increased action potential firing rates of layer 2/3 pyramidal cells in the prefrontal cortex are significantly related to cognitive performance in aged monkeys. *Cereb Cortex* **15**, 409–418.

Chase MH, Engelhardt JK, Adinolfi AM & Chirwa SS (1992). Age-dependent changes in cat masseter nerve: an electrophysiological and morphological study. *Brain Res* **586**, 279–288.

Choi YY, Shamosh NA, Cho SH, De Young CG, Lee MJ, Lee J-M, Kim SI, Cho Z-H, Kim K & Gray JR (2008). Multiple bases of human intelligence revealed by cortical thickness and neural activation. *J Neurosci* **28**, 10323–10329.

Cruikshank SJ, Rose HJ & Metherate R (2002). Auditory thalamocortical synaptic transmission in vitro. *J Neurophysiol* **87**, 361–384.

Dickerson B, Fenstermacher E, Salat D, Wolk D, Maguire R, Desikan R, Pacheco J, Quinn B, Van der Kouwe A & Greve D (2008). Detection of cortical thickness correlates of cognitive performance: reliability across MRI scan sessions, scanners, and field strengths. *NeuroImage* **39**, 10–18.

Dumitriu D, Hao J, Hara Y, Kaufmann J, Janssen WG, Lou W, Rapp PR & Morrison JH (2010). Selective changes in thin spine density and morphology in monkey prefrontal cortex correlate with aging-related cognitive impairment. *J Neurosci* **30**, 7507–7515.

Fortune B, Reynaud J, Cull G, Burgoyne CF & Wang L (2014). The effect of age on optic nerve axon counts, SDOCT scan quality, and peripapillary retinal nerve fiber layer thickness measurements in rhesus monkeys. *Transl Vis Sci Technol* **3**, 2.

Gazzaley A, Clapp W, Kelley J, McEvoy K, Knight RT & D'Esposito M (2008). Age-related top-down suppression deficit in the early stages of cortical visual memory processing. *Proc Natl Acad Sci USA* **105**, 13122–13126.

Gazzaley A & D'Esposito M (2007). Top-down modulation and normal aging. *Ann N Y Acad Sci* **1097**, 67–83.

Gerich FJ, Funke F, Hildebrandt B, Fasshauer M & Müller M (2009). H(2)O(2)-mediated modulation of cytosolic signaling and organelle function in rat hippocampus. *Pflugers Arch* **458**, 937–952.

Gold JR & Bajo VM (2014). Insult-induced adaptive plasticity of the auditory system. *Front Neurosci* **8**, 110.

Gutierrez A, Khan ZU, Morris SJ & De Blas AL (1994). Age-related decrease of $GABA_A$ receptor subunits and glutamic acid decarboxylase in the rat inferior colliculus. *J Neurosci* **14**, 7469–7477.

Hackett TA, Barkat TR, O'Brien BM, Hensch TK & Polley DB (2011). Linking topography to tonotopy in the mouse auditory thalamocortical circuit. *J Neurosci* **31**, 2983–2995.

Haug H, Kühl S, Mecke E, Sass N & Wasner K (1983). The significance of morphometric procedures in the investigation of age changes in cytoarchitectonic structures of human brain. *J Hirnforsch* **25**, 353–374.

Healey MK, Campbell KL & Hasher L (2008). Cognitive aging and increased distractibility: costs and potential benefits. In *Progress in Brain Research*, ed. Wayne S, Sossin J-CLVFC & Sylvie B, pp. 353–363. Elsevier, Amsterdam.

Hébert S, Fournier P & Noreña A (2013). The auditory sensitivity is increased in tinnitus ears. *J Neurosci* **33**, 2356–2364.

Helfer KS & Freyman RL (2008). Aging and speech-on-speech masking. *Ear Hear* **29**, 87.

Hof PR, Duan H, Page TL, Einstein M, Wicinski B, He Y, Erwin JM & Morrison JH (2002). Age-related changes in GluR2 and NMDAR1 glutamate receptor subunit protein immunoreactivity in corticocortically projecting neurons in macaque and patas monkeys. *Brain Res* **928**, 175–186.

Hughes LF, Turner JG, Parrish JL & Caspary DM (2010). Processing of broadband stimuli across A1 layers in young and aged rats. *Hear Res* **264**, 79–85.

Humes LE (2007). The contributions of audibility and cognitive factors to the benefit provided by amplified speech to older adults. *J Am Acad Audiol* **18**, 590–603.

Jacobson M, Kim S, Romney J, Zhu X & Frisina RD (2003). Contralateral suppression of distortion-product otoacoustic emissions declines with age: a comparison of findings in CBA mice with human listeners. *Laryngoscope* **113**, 1707–1713.

Jankelowitz SK, McNulty PA & Burke D (2007). Changes in measures of motor axon excitability with age. *Clin Neurophysiol* **118**, 1397–1404.

Kiernan MC, Lin CS, Andersen KV, Murray NM & Bostock H (2001). Clinical evaluation of excitability measures in sensory nerve. *Muscle Nerve* **24**, 883–892.

Kotak VC, Fujisawa S, Lee FA, Karthikeyan O, Aoki C & Sanes DH (2005). Hearing loss raises excitability in the auditory cortex. *J Neurosci* **25**, 3908–3918.

Lindquist CE, Laver DR & Birnir B (2005). The mechanism of SR95531 inhibition at GABA receptors examined in human $\alpha_1\beta_1$ and $\alpha_1\beta_1\gamma_{2S}$ receptors. *J Neurochem* **94**, 491–501.

Ling LL, Hughes LF & Caspary DM (2005). Age-related loss of the GABA synthetic enzyme glutamic acid decarboxylase in rat primary auditory cortex. *Neuroscience* **132**, 1103–1113.

Llano DA, Slater BJ, Lesicko AM & Stebbings KA (2014). An auditory colliculothalamocortical brain slice preparation in mouse. *J Neurophysiol* **111**, 197–207.

Llano DA, Theyel BB, Mallik AK, Sherman SM & Issa NP (2009). Rapid and sensitive mapping of long-range connections in vitro using flavoprotein autofluorescence imaging combined with laser photostimulation. *J Neurophysiol* **101**, 3325–3340.

Llano DA, Turner J & Caspary DM (2012). Diminished cortical inhibition in an aging mouse model of chronic tinnitus. *J Neurosci* **32**, 16141–16148.

Longenecker RJ & Galazyuk AV (2011). Development of tinnitus in CBA/CaJ mice following sound exposure. *J Assoc Res Otolaryngol* **12**, 647–658.

Luebke J, Chang Y-M, Moore T & Rosene D (2004). Normal aging results in decreased synaptic excitation and increased synaptic inhibition of layer 2/3 pyramidal cells in the monkey prefrontal cortex. *Neuroscience* **125**, 277–288.

Luebke JI & Chang YM (2007). Effects of aging on the electrophysiological properties of layer 5 pyramidal cells in the monkey prefrontal cortex. *Neuroscience* **150**, 556–562.

Magnusson KR (2012). Aging of the NMDA receptor: from a mouse's point of view. *Future Neurol* **7**, 627–637.

Masliah E, Mallory M, Hansen L, DeTeresa R & Terry R (1993). Quantitative synaptic alterations in the human neocortex during normal aging. *Neurology* **43**, 192–192.

Matsubara M, Ranji M, Leshnower BG, Noma M, Ratcliffe SJ, Chance B, Gorman RC & Gorman JH, 3rd (2010). In vivo fluorometric assessment of cyclosporine on mitochondrial function during myocardial ischemia and reperfusion. *Ann Thorac Surg* **89**, 1532–1537.

Mayevsky A (1984). Brain NADH redox state monitored in vivo by fiber optic surface fluorometry. *Brain Res reviews* **7**, 49–68.

Middleton JW, Kiritani T, Pedersen C, Turner JG, Shepherd GM & Tzounopoulos T (2011). Mice with behavioral evidence of tinnitus exhibit dorsal cochlear nucleus hyperactivity because of decreased GABAergic inhibition. *Proc Natl Acad Sci USA* **108**, 7601–7606.

Milad MR, Quinn BT, Pitman RK, Orr SP, Fischl B & Rauch SL (2005). Thickness of ventromedial prefrontal cortex in humans is correlated with extinction memory. *Proc Natl Acad Sci USA* **102**, 10706–10711.

Milbrandt JC, Albin RL & Caspary DM (1994). Age-related decrease in $GABA_B$ receptor binding in the Fischer 344 rat inferior colliculus. *Neurobiol Aging* **15**, 699–703.

Milbrandt JC, Holder TM, Wilson MC, Salvi RJ & Caspary DM (2000). GAD levels and muscimol binding in rat inferior colliculus following acoustic trauma. *Hear Res* **147**, 251–260.

Miller JM, Dolan DF, Raphael Y & Altschuler RA (1997). Interactive effects of aging with noise induced hearing loss. *Scand Audiol Suppl* **48**, 53–61.

Norena AJ (2011). An integrative model of tinnitus based on a central gain controlling neural sensitivity. *Neurosci Biobehav Rev* **35**, 1089–1109.

Ohlemiller KK, Dahl AR & Gagnon PM (2010). Divergent aging characteristics in CBA/J and CBA/CaJ mouse cochleae. *J Assoc Res Otolaryngol* **11**, 605–623.

Ouda L, Nwabueze-Ogbo FC, Druga R & Syka J (2003). NADPH-diaphorase-positive neurons in the auditory cortex of young and old rats. *Neuroreport* **14**, 363–366.

Parthasarathy A, Cunningham PA & Bartlett EL (2010). Age-related differences in auditory processing as assessed by amplitude-modulation following responses in quiet and in noise. *Front Aging Neurosci* **2**, 152.

Parthasarathy A, Datta J, Torres JA, Hopkins C & Bartlett EL (2014). Age-related changes in the relationship between auditory brainstem responses and envelope-following responses. *J Assoc Res Otolaryngol* **15**, 649–661.

Profant O, Balogova Z, Dezortova M, Wagnerova D, Hajek M & Syka J (2013). Metabolic changes in the auditory cortex in presbycusis demonstrated by MR spectroscopy. *Exp Gerontol* **48**, 795–800.

Richardson BD, Ling LL, Uteshev VV & Caspary DM (2013). Reduced $GABA_A$ receptor-mediated tonic inhibition in aged rat auditory thalamus. *J Neurosci* **33**, 1218–1227.

Salat DH, Buckner RL, Snyder AZ, Greve DN, Desikan RS, Busa E, Morris JC, Dale AM & Fischl B (2004). Thinning of the cerebral cortex in aging. *Cereb Cortex* **14**, 721–730.

Schmidt S, Redecker C, Bruehl C & Witte OW (2010). Age-related decline of functional inhibition in rat cortex. *Neurobiol Aging* **31**, 504–511.

Segal M (1982). Changes in neurotransmitter actions in the aged rat hippocampus. *Neurobiol Aging* **3**, 121–124.

Sepehr R, Staniszewski K, Maleki S, Jacobs ER, Audi S & Ranji M (2012). Optical imaging of tissue mitochondrial redox state in intact rat lungs in two models of pulmonary oxidative stress. *J Biomed Opt* **17**, 046010.

Sha S-H, Kanicki A, Dootz G, Talaska AE, Halsey K, Dolan D, Altschuler R & Schacht J (2008). Age-related auditory pathology in the CBA/J mouse. *Hear Res* **243**, 87–94.

Shibuki K, Hishida R, Murakami H, Kudoh M, Kawaguchi T, Watanabe M, Watanabe S, Kouuchi T & Tanaka R (2003). Dynamic imaging of somatosensory cortical activity in the rat visualized by flavoprotein autofluorescence. *J Physiol* **549**, 919–927.

Simon H, Frisina RD & Walton JP (2004). Age reduces response latency of mouse inferior colliculus neurons to AM sounds. *J Acoust Soc Am* **116**, 469–477.

Sowell ER, Peterson BS, Thompson PM, Welcome SE, Henkenius AL & Toga AW (2003). Mapping cortical change across the human life span. *Nat Neurosci* **6**, 309–315.

Staniszewski K, Audi SH, Sepehr R, Jacobs ER & Ranji M (2013). Surface fluorescence studies of tissue mitochondrial

redox state in isolated perfused rat lungs. *Ann Biomed Eng* **41**, 827–836.
Takesian AE, Kotak VC & Sanes DH (2009). Developmental hearing loss disrupts synaptic inhibition: implications for auditory processing. *Future Neurol* **4**, 331–349.
Takesian AE, Kotak VC & Sanes DH (2012). Age-dependent effect of hearing loss on cortical inhibitory synapse function. *J Neurophysiol* **107**, 937–947.
Taylor L & Griffith WH (1993). Age-related decline in cholinergic synaptic transmission in hippocampus. *Neurobiol Aging* **14**, 509–515.
Terry RD, DeTeresa R & Hansen LA (1987). Neocortical cell counts in normal human adult aging. *Ann Neurol* **21**, 530–539.
Thambisetty M, Wan J, Carass A, An Y, Prince JL & Resnick SM (2010). Longitudinal changes in cortical thickness associated with normal aging. *NeuroImage* **52**, 1215–1223.
Tun PA, O'Kane G & Wingfield A (2002). Distraction by competing speech in young and older adult listeners. *Psychol Aging* **17**, 453.
Ueno S, Bracamontes J, Zorumski C, Weiss DS & Steinbach JH (1997). Bicuculline and gabazine are allosteric inhibitors of channel opening of the $GABA_A$ receptor. *J Neurosci* **17**, 625–634.
Yu ZY, Wang W, Fritschy JM, Witte OW & Redecker C (2006). Changes in neocortical and hippocampal $GABA_A$ receptor subunit distribution during brain maturation and aging. *Brain Res* **1099**, 73–81.
Yueh B, Shapiro N, MacLean CH & Shekelle PG (2003). Screening and management of adult hearing loss in primary care: scientific review. *JAMA* **289**, 1976–1985.
Zettel ML, Frisina RD, Haider S-EA & O'Neill WE (1997). Age-related changes in calbindin D-28k and calretinin immunoreactivity in the inferior colliculus of CBA/CaJ and C57Bl/6 mice. *J Comp Neurol* **386**, 92–110.
Zheng QY, Johnson KR & Erway LC (1999). Assessment of hearing in 80 inbred strains of mice by ABR threshold analyses. *Hear Res* **130**, 94–107.

Additional information

Conflict of interest

J.G.T. is the CEO of OtoScience Labs, LLC. This company focuses on hearing contract research and development.

Author contributions

K.A.S, J.G.T, D.M.C and D.A.L studied design/results interpretation. K.A.S performed the experiments. Writing was done by K.A.S and D.A.L. Data analysis was done by K.A.S, H.W.C., A.R. and D.A.L. All authors have approved the final version of the manuscript and agree to be accountable for all aspects of the work. All persons designated as authors qualify for authorship, and all those who qualify for authorship are listed.

Funding

This work was supported by DC012125 as well as the American Federation of Aging Research and the Alzheimer's Association.

Acknowledgements

The authors wish to acknowledge Masha Ranji for her advice with the redox imaging, Xuan Bi from the Illinois Statistics office and John R. Viren for his statistical advice and assistance, Jiarong 'Jerry' Fu for his assistance with MATLAB coding and Patrick Mulligan for his assistance with data processing.